UDC 621.314 https://doi.org/10.20998/2074-272X.2023.3.06

A. Boukadoum, A. Bouguerne, T. Bahi

Direct power control using space vector modulation strategy control for wind energy conversion system using three-phase matrix converter

Introduction. *Wind energy conversion system is getting a lot of attention since, they are provide several advantages, such as cost competitive, environmentally clean, and safe renewable power source as compared with the fossil fuel and nuclear power generation. A special type of induction generator, called a doubly fed induction generator is used extensively for high-power wind energy conversion system. They are used more and more in wind turbine applications due to the advantages of variable speed operation range and its four quadrants active and reactive power capabilities, high energy efficiency, and the improved power quality. Wind energy conversion systems require a good choice of power electronic converters for the improvement of the quality of the electrical energy produced at the generator terminals. There are several power electronics converters that are the most popular such as the two stage back-back converter. Because of the disadvantage of these converters to produce large harmonics distortions, we will choose using of three-phase matrix converter.* ***Purpose.*** *Work presents a direct power control using space vector modulation for a doubly fed induction generator based wind turbine. The main strategy control is to control the active and reactive powers and reduce the harmonic distortion of stator currents for variable wind speed. The* ***novelty*** *of the work is to use a doubly fed induction machine and a three pulses matrix converter to reduce the low cost, volume and the elimination of the grid side converter controller are very attractive aspects of the proposed topology compared to the conventional methods such as back-to-back converters. Simulation* ***results*** *are carried out on a 1.5 MW of wind energy conversion system connected to the grid. The efficiency of the proposed system has been simulated and high results performances are evaluated to show the validity of the proposed control strategy to decouple and control the active and reactive power for different values of wind* speed. References 32, tables 2, figures 15.

Key words: **doubly fed induction generator, matrix converter, wind turbine, direct power control using space vector modulation strategy control, power quality.**

Вступ. *Системам перетворення енергії вітру приділяється велика увага, оскільки вони забезпечують низку переваг, таких як конкурентоспроможність за вартістю, екологічно чисте та безпечне відновлюване джерело енергії порівняно з викопним паливом та виробництвом ядерної енергії. Спеціальний тип асинхронного генератора, що називається асинхронним генератором з подвійним живленням, широко використовується в системах перетворення енергії вітру великої потужності. Вони все більше і більше використовуються у вітряних турбінах через переваги діапазону роботи зі змінною швидкістю та його чотириквадрантних можливостей активної та реактивної потужності, високої енергоефективності та покращеної якості електроенергії. Системи перетворення енергії вітру вимагають хорошого вибору силових електронних перетворювачів для покращення якості електроенергії, що виробляється на клемах генератора. Існує кілька перетворювачів силової електроніки, які є найбільш популярними, наприклад двокаскадний зворотно-зворотний перетворювач. Через те, що ці перетворювачі не створюють великих гармонічних спотворень, ми виберемо використання трифазного матричного перетворювача.* ***Мета***. *У роботі представлено пряме керування потужністю з використанням модуляції просторового вектора для вітрової турбіни на основі асинхронного генератора з подвійним живленням. Основною стратегією управління є управління активною та реактивною потужністю та зниження гармонійних спотворень струмів статора при змінній швидкості вітру.* ***Новизна*** *роботи полягає у використанні асинхронної машини з подвійним живленням і триімпульсного матричного перетворювача для зниження вартості, об'єму та усунення контролера перетворювача з боку мережі, що є дуже привабливими аспектами пропонованої топології у порівнянні зі звичайними методами, такими як зустрічно-зворотні перетворювачі.* ***Результати*** *моделювання отримані на системі перетворення енергії вітру потужністю 1,5 МВт, підключеної до мережі. Ефективність запропонованої системи була змодельована, а високі результати оцінені, щоб показати обґрунтованість запропонованої стратегії управління для поділу та управління активною та реактивною потужністю для різних значень швидкості вітру.* Бібл. 32, табл. 2, рис. 15.

Ключові слова: **асинхронний генератор з подвійним живленням, матричний перетворювач, вітряна турбіна, пряме керування потужністю з використанням стратегії просторово-векторної модуляції, якість електроенергії.**

1. Introduction. Nowadays, the use of renewable energy system in modern production of electrical energy has exponentially increased due to the increase in greenhouse gas concentrations in the atmosphere, which are extremely destructive to our planet [1]. Wind energy has grown faster than any other source of renewable energy [2]. Wind energy can help reduce total air pollution and carbon dioxide emissions, this generator is one of the rapidly expanding renewable energy sources with a 93 GW capacity addition in 2020 [3], it has become a suitable solution for producing clean energy and is currently the quickest developing source when correlated with other sustainable power sources [4]. Nonetheless, the use of available energy depends on weather conditions such as wind speed and its integration produces volatility in the power system. Integrating renewable energies with network connection, intelligent control, and storage systems could result in a change in generating electricity and reducing. Given current trends and the best available scientific evidence, mankind probably needs to reduce total emissions by at least 80 % since 2050 [5]. Yet each day emissions continue to grow [6]. Wind energy conversion system (WECS) is getting a lot of attention since, they are provide several advantages, such as cost competitive, environmentally clean, and safe renewable power source as compared with the fossil fuel and nuclear power generation. A special type of induction generator, called a doubly fed induction generator (DFIG), is used extensively for high-power wind applications. They are used more and more in wind turbine applications due to the advantages of variable speed operation range and its four quadrants active and reactive power capabilities, high energy efficiency, and the improved power quality [7, 8]. WECSs require a good choice of power electronic converters for the improvement of the quality of the electrical energy produced at the generator terminals. There are several power electronics converters that are the most popular such as the two stage back-back converter and cycloconverter [9, 10]. Because of the disadvantage of these converters to produce large harmonics, we will choose using of direct matrix converter. The system under study is depicted in Fig. 1.

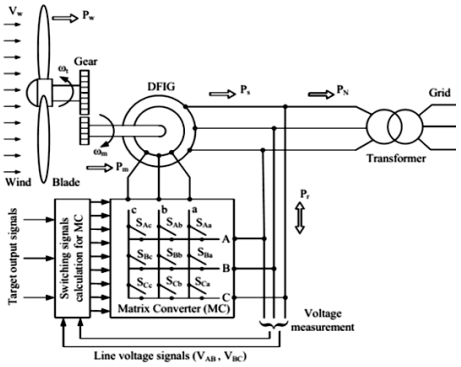

Fig. 1. WECS connected to the grid

It is composed of DFIG-wind turbine connected to the grid via a direct matrix converter (DMC). Wind turbines using a DFIG consist of a wound rotor induction generator and a three phase direct matrix converter. The stator winding is connected directly to the 50 Hz grid while the rotor is fed at variable frequency through the direct matrix converter [11, 12]. The DFIG technology allows extracting maximum energy from the wind for low wind speeds by optimizing the turbine speed, while minimizing mechanical stresses on the turbine during gusts of wind. In this study the variable wind speed is maintained at 9 m/s, 15 m/s and 11 m/s. Simulation results are carried out on a 1.5 MW DFIG WECS connected to the 575 V of voltage grid. The reactive power produced by the wind turbine is regulated at zero MVar. The paper is organized as follows: In section 2, the model of the wind turbine is presented. Next, the modeling of DFIG system is detailed in section 3. In section 4, mathematical modeling of a DMC is discussed. In section 5, the procedure of direct power control using space vector modulation (DPC-SVM) based direct matrix converter is explained. The simulation results are presented in section 6. Finally, section 7 concludes this study.

2. Wind turbine model. Wind energy can only extract a small part of the power from the wind, which is limited by the Betz limit to a maximum of 59 %. This quantity is described by the turbine power coefficient C_p, which is dependent on the blade pitch angle β and the peak speed ratio λ. The mechanical power of the wind turbine extracted from the wind is given by:

$$P_W = \frac{1}{2}\cdot\rho\cdot\pi\cdot R^2\cdot C_p(\lambda,\beta)\cdot V^3, \quad (1)$$

where C_p is the power coefficient of the wind turbine; β is the blade pitch angle; λ is the tip speed ratio; ρ is the density of air; R is the rotor radius of wind, m; V is the wind speed, m/s.

The tip speed ratio λ is calculated from the actual values of rotor speed and wind speed V according to:

$$\lambda = \frac{R\cdot\Omega_W}{V}, \quad (2)$$

where Ω_W is the angular velocity of rotor, rad/s.

From summaries achieved on a wind of 1.5 MW, the expression of the power coefficient for this type of turbine can be approximated by the following expression:

$$C_p(\lambda,\beta) = C_1\cdot\left(\frac{C_2}{\lambda_i} - C_3\cdot\beta - C_4\right)\cdot e^{\left(\frac{C_5}{\lambda_i}\right)} + C_6\cdot\lambda. \quad (3)$$

The parameter $1/\lambda_i$ in (3) is defined as

$$\frac{1}{\lambda_i} = \frac{1}{\lambda + 0.008\cdot\beta} - \frac{0.035}{1+\beta^2}. \quad (4)$$

The proposed coefficients are equal to:
$C_1 = 0.5176$, $C_2 = 116$, $C_3 = 0.4$, $C_4 = 5$, $C_5 = 2$, $C_6 = 0.0068$.

The gearbox is installed between the turbine and the generator to transform slow speed wind turbine rotation to higher speed required by the generator [13]. Neglecting the gearbox losses, the mechanical torque and shaft speed of the wind turbine referred to the generator side of the gearbox are given by:

$$T_g = \frac{T_W}{G}; \quad \Omega_g = \Omega_W\cdot G, \quad (5)$$

where T_W, T_g are the wind turbine aerodynamic and generator electromagnetic torques, N·m.

The resulting block diagram of the wind turbine model is presented in Fig. 2.

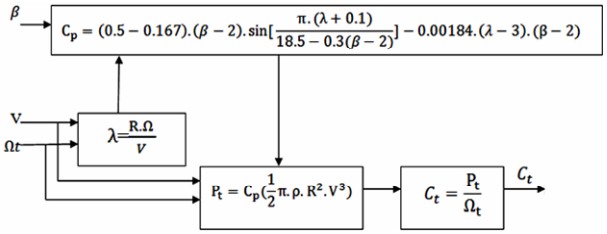

Fig. 2. Block diagram of the wind turbine model

Figure 3 illustrated the curves of power coefficient versus the tip-speed ratio for different values of the pitch angle. We can see in this figure that the optimal power coefficient of C_p is 0.48 for a speed ration at 8 and β equal to 0°.

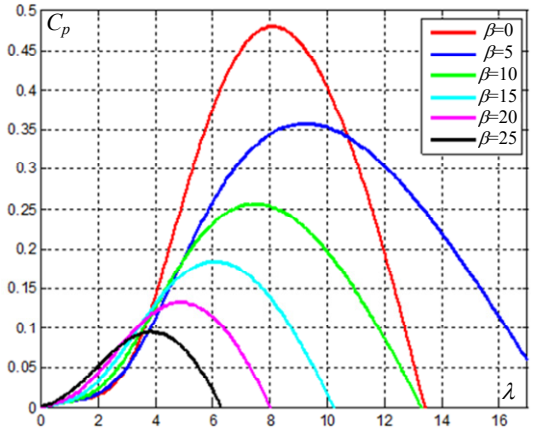

Fig. 3. Power coefficients for different values of β

3. DFIG model. By choosing a *d-q* reference frame synchronized with the stator flux, the electrical equations of the DFIG are written as follows:

$$\begin{cases} \frac{\mathrm{d}}{\mathrm{d}t}\varphi_{sd} = V_{sd} - R_s i_{sd} + \omega_s\varphi_{sq}; \\ \frac{\mathrm{d}}{\mathrm{d}t}\varphi_{sq} = V_{sq} - R_s i_{sq} + \omega_s\varphi_{sd}; \\ \frac{\mathrm{d}}{\mathrm{d}t}\varphi_{rd} = V_{rd} - R_r i_{rd} + (\omega_s - \omega)\cdot\varphi_{rq}; \\ \frac{\mathrm{d}}{\mathrm{d}t}\varphi_{rq} = V_{rq} - R_r i_{rq} - (\omega_s - \omega)\cdot\varphi_{rd}, \end{cases} \quad (6)$$

where V_{sd}, V_{sq}, i_{sd}, i_{sq} are the stator voltages and currents in the synchronous reference frame, respectively; V_{rd}, V_{rq}, i_{rd}, i_{rq} are the rotor voltages and currents in the synchronous reference frame, respectively; ω_s is the stator

angular frequency; ω is the slip angular speed; R_s is the stator resistance; φ_s, φ_r are the stator and rotor fluxes.

The stator and rotor flux can be expressed as

$$\begin{cases} \varphi_{sd} = L_s i_{sd} + M i_{rd}; \\ \varphi_{sq} = L_s i_{sq} + M i_{rq}; \\ \varphi_{rd} = L_r i_{rd} + M i_{sd}; \\ \varphi_{rq} = L_r i_{rq} + M i_{sq}. \end{cases} \quad (7)$$

The expressions of real and reactive power are given by:

$$\begin{cases} P_s = V_{sd} i_{sd} + V_{sq} i_{sq}; \\ Q_s = V_{sq} i_{sd} - V_{sd} i_{sq}; \\ P_r = V_{rd} i_{rd} + V_{rq} i_{rq}; \\ Q_r = V_{rq} i_{rd} - V_{rd} i_{rq}. \end{cases} \quad (8)$$

The control strategy, using the model of DFIG in (d-q) reference axis is the vector stator flux aligned with d-axis. So, by setting the quadratic component of the stator flux to the null value and by neglecting the stator resistance, the voltage equations of the stator windings can be simplified in steady state as:

$$\begin{cases} V_{sd} = \dfrac{\mathrm{d}\varphi_{sd}}{\mathrm{d}t} = 0; \\ V_{sq} = \omega_s \cdot \varphi_{sd} = V_s. \end{cases} \quad (9)$$

Hence, the relationship between the stator and rotor currents can be written as follows:

$$\begin{cases} i_{sd} = \dfrac{\varphi_s}{L_s} - \dfrac{L_m}{L_s} \cdot i_{rd}; \\ i_{sq} = -\dfrac{L_m}{L_s} \cdot i_{rq}. \end{cases} \quad (10)$$

From (8), (9), we can write:

$$\begin{cases} \varphi_{rd} = (L_r - \dfrac{M^2}{L_s}) \cdot i_{rd} + \dfrac{M V_s}{\omega_s L_s}; \\ \varphi_{rd} = (L_r - \dfrac{M^2}{L_s}) \cdot i_{rd}. \end{cases} \quad (11)$$

The expression of the stator and rotor voltage is given by:

$$\begin{cases} V_{sd} = \dfrac{R_s}{L_s} \varphi_{sd} - \dfrac{R_s}{L_s} M i_{rd}; \\ V_{sq} = -\dfrac{R_s}{L_s} \varphi_{rq} + \omega_s \varphi_{rd}; \\ V_{rd} = R_r i_{rd} + \sigma \cdot L_r \dfrac{\mathrm{d}i_{rd}}{\mathrm{d}t} + e_{rd}; \\ V_{rq} = R_r i_{rq} + \sigma \cdot L_r \dfrac{\mathrm{d}i_{rq}}{\mathrm{d}t} + e_{rd} + e_{\varphi}, \end{cases} \quad (12)$$

where:

$$\begin{cases} e_{rd} = \dfrac{R_s}{L_s} \varphi_{sd} - \dfrac{R_s}{L_s} M i_{rd}; \\ e_{rq} = -\dfrac{R_s}{L_s} \varphi_{rq} + \omega_s \varphi_{rd}; \\ e_{\varphi} = \omega_r \cdot \dfrac{M}{L_s} \cdot \varphi_{sd}; \\ \sigma = 1 - (\dfrac{M}{\sqrt{L_s L_r}})^2. \end{cases} \quad (13)$$

Stator real and reactive powers are described by:

$$P_s = g \cdot \frac{V_s M}{L_s} \cdot i_{rq}; \quad Q_s = g \cdot \frac{V_s M}{L_s} \cdot i_{rd}. \quad (14)$$

The electromagnetic torque is as follows:

$$T_{em} = -P \cdot \frac{M}{L_s} \cdot \varphi_{sd} \cdot i_{rq}. \quad (15)$$

4. Matrix converter (MC) is a DMC used to convert AC supply voltages into variable magnitude and frequency output voltages [14, 15] (Fig. 4). Three phases MC consists of array of nine IGBTs switches that are switched on and off in order to provide variable sinusoidal voltage and frequency to the load [8], in this type of converter there is no need to the intermediate DC link power circuit and this means no large energy storing capacitors [8-10]. This will increase the system reliability and reduce the weight and volume for such converters [16, 17]. This converter is proposed as an effective replacement for the WECS fed by back-to-back converter. The input voltages and currents can be given as:

$$V_i(t) = V_{i\max} \begin{bmatrix} \sin(\omega_i t) \\ \sin(\omega_i t - 2\pi/3) \\ \sin(\omega_i t - 4\pi/3) \end{bmatrix}. \quad (16)$$

$$i_i(t) = I_{i\max} \begin{bmatrix} \sin(\omega_i t + \varphi_i) \\ \sin(\omega_i t - 2\pi/3 + \varphi_i) \\ \sin(\omega_i t - 4\pi/3 + \varphi_i) \end{bmatrix}. \quad (17)$$

where $i = \{A, B, C\}$ is the name of the input phase.

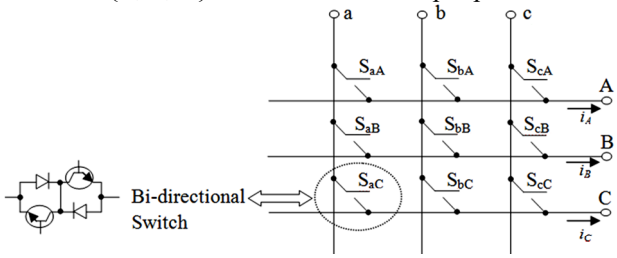

Fig. 4. Symbol of three phase matrix converter

The matrix converter will be designed and controlled in such a manner that the fundamental of the output voltages are:

$$V_j(t) = V_{j\max} \begin{bmatrix} \sin(\omega_i t) \\ \sin(\omega_i t - 2\pi/3) \\ \sin(\omega_i t - 4\pi/3) \end{bmatrix}. \quad (18)$$

$$i_j(t) = I_{j\max} \begin{bmatrix} \sin(\omega_i t + \varphi_j) \\ \sin(\omega_i t - 2\pi/3 + \varphi_j) \\ \sin(\omega_i t - 4\pi/3 + \varphi_j) \end{bmatrix}, \quad (19)$$

where $j = \{a, b, c\}$ is the name of the output phase.

Ratio q is the ratio voltage between, its value cannot exceed 0.866 and cannot be negative [18, 19]:

$$q = V_{j\max} / V_{i\max}. \quad (20)$$

The switching function of a single switch is defined as follows:

$$S_{ij}(t) = \begin{cases} 0 \text{ is } S_{ij} \text{ is open;} \\ 1 \text{ is } S_{ij} \text{ is closed,} \end{cases} \quad (21)$$

where S_{ij} is the bi-directional power switch of matrix converter (see Fig. 4).

The input/output relationships of voltages and currents are related to the states of the nine switches, and can be written in matrix form as:

$$\begin{cases} V_j(t) = M(t) \cdot V_i(t); \\ i_i(t) = M(t)^t \cdot i_j(t). \end{cases} \quad (22)$$

The matrix $M(t)^t$ is the transpose of the matrix $M(t)$;

$$M(t) = \begin{vmatrix} m_{Aa}(t) & m_{Ba}(t) & m_{Ca}(t) \\ m_{Ab}(t) & m_{Bb}(t) & m_{Cb}(t) \\ m_{Ac}(t) & m_{Bc}(t) & m_{Cc}(t) \end{vmatrix}. \quad (23)$$

The variables $m_{ij}(t)$ are the duty-cycles of the 9 switches and can be represented by:

$$m_{ij}(t) = \frac{1}{T}\int_0^T S_{ij}(t)\mathrm{d}t, \quad (24)$$

where $0 \le m_{ij}(t) \le 1$; T is the switching period.

5. Control of matrix converter. There are a number of possible modulation techniques that can be used for matrix converter control. The optimal modulation strategy should minimize the input current and output voltage harmonic distortion and device power losses. The most relevant control and modulation methods developed for the MCs are the Venturini method, the scalar method developed by Roy and the space-vector modulation (SVM) [20-24]. In this work the SVM method is preferred because it deals with scalar quantities rather than vectors, and this is important when controlling WECS. The SVM had previously been used for inverter control [25] proposed the use of SVM for matrix converters, this strategy control is based on the space vector representation of the input currents and output voltages at any time [26].

$$\vec{V}_j(t) = \frac{2}{3}(v_a + a \cdot v_b + a^2 \cdot v_c) = V_0 e^{\alpha_i t}; \quad (25)$$

$$\vec{i}_i(t) = \frac{2}{3}(i_a + a \cdot i_b + a^2 \cdot i_c) = I_i e^{\beta_i t}, \quad (26)$$

where $a = e^{j\frac{2\pi}{3}}$.

For the three-phase matrix converter, there are 27 possible switching configurations. The first 18 switching configurations determine an output voltage vector and an input current vector and will be named «active configurations». The last 3 switching configurations determine zero input current and output voltage vectors and will be named «zero configurations». The required modulation duty cycles for the switching configurations are giving by the following equation [21-23, 25]. These switching states and the output voltages and input current vectors are presented in Table 1. The sum of the absolute values of the four duty-cycles must be lower than unity.

In the control strategy of the WECS, the DPC-SVM uses 2 control loops with PI controllers, these inner control loops regulate the active and reactive power of AC grid. The estimated values of active and reactive AC grid power are compared with the real and reactive powers references [27-29]. To ensure a pure active power exchange from the wind generator and maintain the reactive power exchange to the grid.

The dynamic model of grid side electrical circuits is presented as [29-32]:

$$\begin{cases} V_{sd} = R_s i_{sd} + L_s \dfrac{\mathrm{d}i_{sd}}{\mathrm{d}t} - \omega_s L_s i_{sq} + e_{csd}; \\ V_{sq} = R_s i_{sq} + L_s \dfrac{\mathrm{d}i_{sq}}{\mathrm{d}t} - \omega_s L_s i_{sd} + e_{csq}. \end{cases} \quad (27)$$

The active and reactive power estimator as:

$$\begin{cases} P_{sd} = \dfrac{3}{2}(v_{sd} i_{sd} + v_{sq} i_{sq}); \\ Q_{sq} = \dfrac{3}{2}(v_{sq} i_{sd} - v_{sd} i_{sq}). \end{cases} \quad (28)$$

Table 1

Switching configurations

N°	Combination	$\vec{V}_0(t)$	$\vec{i}_i(t)$
1	S_{Aa}, S_{Bb}, S_{Cb}	$(2/3)\cdot V_{ab}\cdot e^{j0}$	$(2/\sqrt{3})\cdot i_A \cdot e^{-j\pi/6}$
2	S_{Ab}, S_{Ba}, S_{Ca}	$-(2/3)\cdot V_{ab}\cdot e^{j0}$	$-(2/\sqrt{3})\cdot i_A \cdot e^{-j\pi/6}$
3	S_{Ab}, S_{Bc}, S_{Cc}	$(2/3)\cdot V_{bc}\cdot e^{j0}$	$(2/\sqrt{3})\cdot i_A \cdot e^{j\pi/2}$
4	S_{Ac}, S_{Bb}, S_{Cb}	$-(2/3)\cdot V_{bc}\cdot e^{j0}$	$-(2/\sqrt{3})\cdot i_A \cdot e^{j\pi/2}$
5	S_{Ac}, S_{Ba}, S_{Ca}	$(2/3)\cdot V_{ca}\cdot e^{j0}$	$(2/\sqrt{3})\cdot i_A \cdot e^{j7\pi/6}$
6	S_{Aa}, S_{Bc}, S_{Cc}	$-(2/3)\cdot V_{ca}\cdot e^{j0}$	$-(2/\sqrt{3})\cdot i_A \cdot e^{j7\pi/6}$
7	S_{Ab}, S_{Ba}, S_{Cb}	$(2/3)\cdot V_{ab}\cdot e^{j2\pi/3}$	$(2/\sqrt{3})\cdot i_B \cdot e^{-j\pi/6}$
8	S_{Aa}, S_{Bb}, S_{Ca}	$-(2/3)\cdot V_{ab}\cdot e^{j2\pi/3}$	$-(2/\sqrt{3})\cdot i_B \cdot e^{-j\pi/6}$
9	S_{Ac}, S_{Bb}, S_{Cc}	$(2/3)\cdot V_{bc}\cdot e^{j2\pi/3}$	$(2/\sqrt{3})\cdot i_B \cdot e^{j\pi/2}$
10	S_{Ab}, S_{Bc}, S_{Cb}	$-(2/3)\cdot V_{bc}\cdot e^{j2\pi/3}$	$-(2/\sqrt{3})\cdot i_B \cdot e^{j\pi/2}$
11	S_{Aa}, S_{Bc}, S_{Ca}	$(2/3)\cdot V_{ca}\cdot e^{j2\pi/3}$	$(2/\sqrt{3})\cdot i_B \cdot e^{j7\pi/6}$
12	S_{Ac}, S_{Ba}, S_{Cc}	$-(2/3)\cdot V_{ca}\cdot e^{j2\pi/3}$	$-(2/\sqrt{3})\cdot i_B \cdot e^{j7\pi/6}$
13	S_{Ab}, S_{Bb}, S_{Ca}	$(2/3)\cdot V_{ab}\cdot e^{j4\pi/3}$	$(2/\sqrt{3})\cdot i_C \cdot e^{-j\pi/6}$
14	S_{Aa}, S_{Ba}, S_{Cb}	$-(2/3)\cdot V_{ab}\cdot e^{j4\pi/3}$	$-(2/\sqrt{3})\cdot i_C \cdot e^{-j\pi/6}$
15	S_{Ac}, S_{Bc}, S_{Cb}	$(2/3)\cdot V_{bc}\cdot e^{j4\pi/3}$	$(2/\sqrt{3})\cdot i_C \cdot e^{j\pi/2}$
16	S_{Ab}, S_{Bb}, S_{Cc}	$-(2/3)\cdot V_{bc}\cdot e^{j4\pi/3}$	$-(2/\sqrt{3})\cdot i_C \cdot e^{j\pi/2}$
17	S_{Aa}, S_{Ba}, S_{Cc}	$(2/3)\cdot V_{ca}\cdot e^{j4\pi/3}$	$(2/\sqrt{3})\cdot i_C \cdot e^{j7\pi/6}$
18	S_{Ac}, S_{Bc}, S_{Ca}	$-(2/3)\cdot V_{ca}\cdot e^{j4\pi/3}$	$-(2/\sqrt{3})\cdot i_C \cdot e^{j7\pi/6}$
19	S_{Aa}, S_{Ab}, S_{Ac}	0	–
20	S_{Ba}, S_{Bb}, S_{Bc}	0	–
21	S_{Ca}, S_{Cb}, S_{Cc}	0	–

6. Simulation results. The simulation of wind system based on DFIG with the considered control systems 1 has been implemented using Simulink/MATLAB (Fig. 5).

The parameters of proposed conversion system are shown in Table 2.

Table 2

System parameters

Parameters, units	Values
Grid frequency f_S, Hz	50
Grid voltage V_{srms}, V	575
Voltage V_{rrms}, V	575
IGBTs switch frequency (SVM), kHz	6
Power P_n, MW	1.5
Voltage (line-line) V_{nrms}, V	575
Stator resistance R_s, Ω	0.01965
Stator Inductance L_s, H	0.0397
Rotor resistance R_s, Ω	0.01909
Rotor Inductance L_s, H	0.0397
Mutual inductance L_m, H	1.354
Inertia J, kg·m^2	0.09526
Flux linkage Φ_f, Wb	0.05479

The obtained simulation results of considered WECS are presented in Fig. 6–8. The considered control of whole system has been tested for the wind speed during the period of the 3 s, while, the average wind speed has been adopted for different average values at 9 m/s, 11 m/s and 15 m/s (Fig. 6).

Figures 7, 8 present the responses of speed rotor and electromagnetic torque compared to the mechanical torque. It can be seen, that the electromagnetic torque T_{em} is accurately adjusted to the mechanical torque.

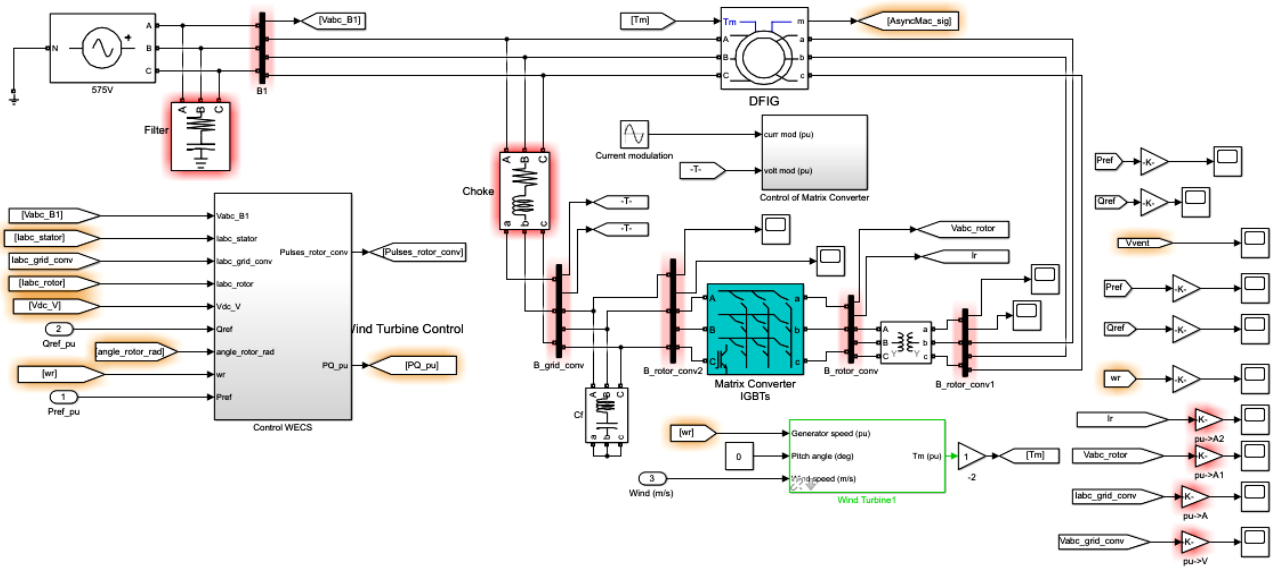

Fig. 5. Simulink model of WECS

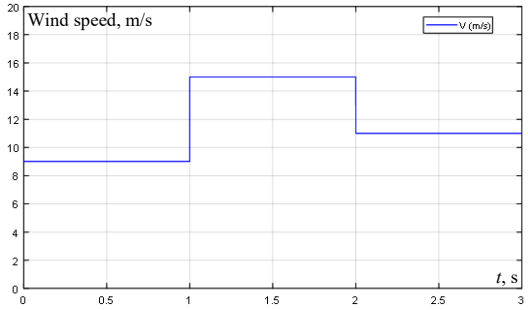

Fig. 6. Wind speed

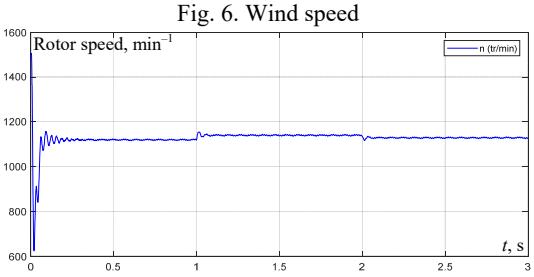

Fig. 7. Rotor speed of DFIG

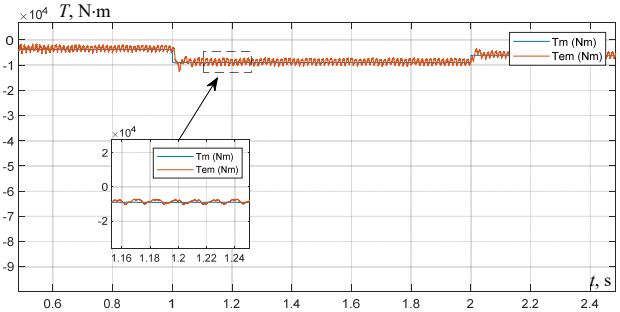

Fig. 8. Electromagnetic torque and its reference

So, the considered control system allows fast responses of the electromagnetic torque T_{em} of DFIG during temporary time variations of the wind speed.

The waveform of output currents (rotor currents of DFIG) and input currents of matrix converter are practically changing according to variations of wind speed (see Fig. 9, 10). We can see that these currents are sinusoidal. Figures 11, 12 display the three-phase voltages and current injected to the grid by the conversion system controlled by DPC-SVM strategy. It can be seen, that this current has a sinusoidal form and changing according to the variations of wind speed.

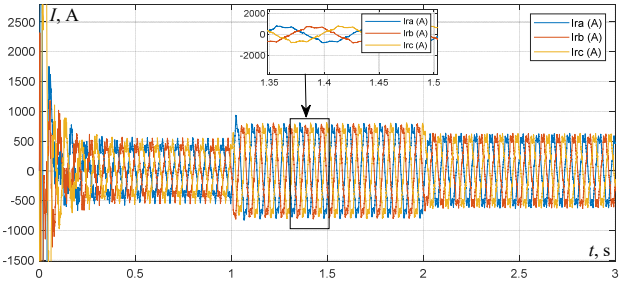

Fig. 9. Rotor currents (output currents of MC)

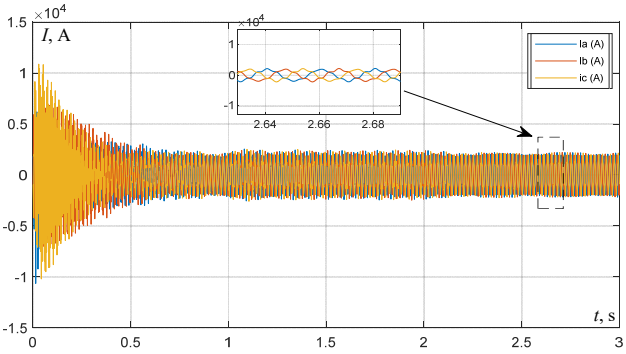

Fig. 10. Input currents of MC

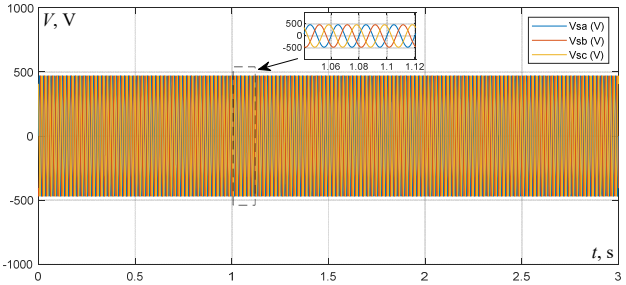

Fig. 11. Stator voltages connected to the grid

Figure 13 shows the grid voltage and current delivered by the generating system. It can be seen that the voltage is in phase opposition with the current, which proves that the proposed system drives with unitary factor power. Finally, Fig. 14, 15 present the active and reactive powers injected to the grid, controlled via the proposed DPC-SVM.

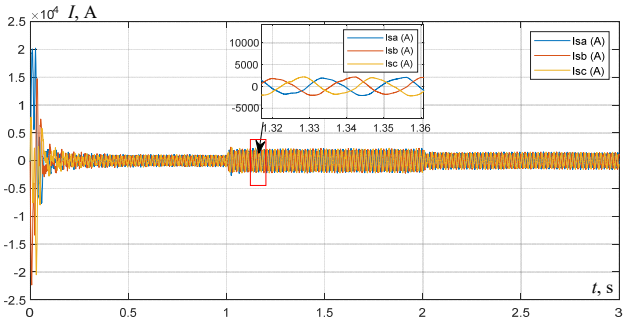

Fig. 12. Stator currents connected to the grid

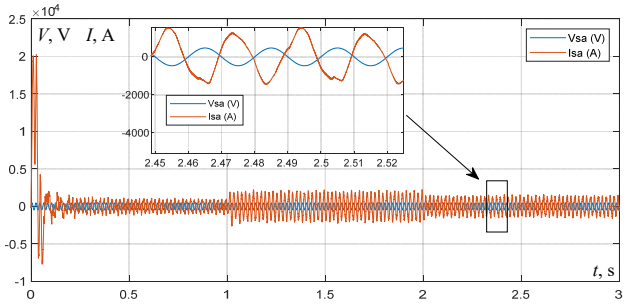

Fig. 13. Waveforms of grid phase voltage and current

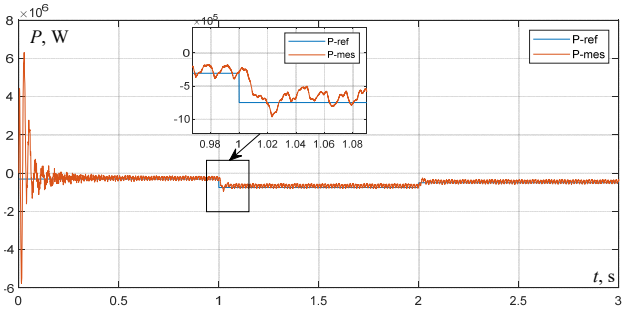

Fig. 14. Active power and its reference connected to the grid

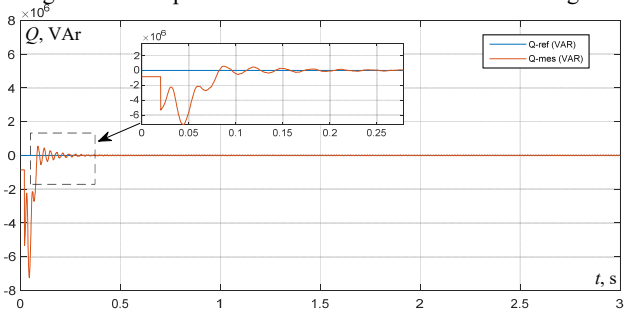

Fig. 15. Reactive power and its reference connected to the grid

We can conclude that, under the proposed control algorithm, the grid power amounts track their references values with smooth profiles. Also, from these figures, it can be noticed, that only the active power generated by the proposed system is fully delivered to the AC grid, while the reactive power is controlled to be zero.

7. Conclusions. In this paper, a new proposed doubly fed induction generator of wind energy conversion system based direct matrix converter connected to the grid has been presented. In this study, the conventional back-to back converters has been replaced by a direct matrix converter using direct power control using space vector modulation strategy control. The advantage in the proposed scheme is that the DC-link capacitors voltage and the grid side converter have been eliminated. In order to control the active and reactive power injected to the grid a direct power control using space vector modulation strategy control have been explored. This technique eliminates the lookup table and reduces the grid powers and currents harmonics as well. In addition, the direct power control using space vector modulation strategy control guarantees good dynamic response and provides sinusoidal line currents. We can confirm that the direct matrix converter presents an interesting alternative for the variable wind speed. The simulation results are satisfactory, have a good performance and good control proprieties between measured and reference quantities. The results encourage a further development of this study to obtain clean energy.

Conflict of interest. The authors declare that they have no conflicts of interest.

REFERENCES

1. Bistline J., Abhyankar N., Blanford G., Clarke L., Fakhry R., McJeon H., Reilly J., Roney C., Wilson T., Yuan M., Zhao A. Actions for reducing US emissions at least 50% by 2030. *Science*, 2022, vol. 376, no. 6596, pp. 922-924. doi: https://doi.org/10.1126/science.abn0661.

2. Williams J.H., DeBenedictis A., Ghanadan R., Mahone A., Moore J., Morrow W.R., Price S., Torn M.S. The Technology Path to Deep Greenhouse Gas Emissions Cuts by 2050: The Pivotal Role of Electricity. *Science*, 2012, vol. 335, no. 6064, pp. 53-59. doi: https://doi.org/10.1126/science.1208365.

3. Pfenninger S., Keirstead J. Comparing concentrating solar and nuclear power as baseload providers using the example of South Africa. *Energy*, 2015, vol. 87, pp. 303-314. doi: https://doi.org/10.1016/j.energy.2015.04.077.

4. Boopathi K., Ramaswamy S., Kirubakaran V., Uma K., Saravanan G., Thyagaraj S., Balaraman K. Economic investigation of repowering of the existing wind farms with hybrid wind and solar power plants: a case study. *International Journal of Energy and Environmental Engineering*, 2021, vol. 12. no. 4, pp. 855-871. doi: https://doi.org/10.1007/s40095-021-00391-3.

5. Staffell I., Pfenninger S. The increasing impact of weather on electricity supply and demand. *Energy*, 2018, vol. 145, pp. 65-78. doi: https://doi.org/10.1016/j.energy.2017.12.051.

6. Sureshkumar K., Ponnusamy V. Hybrid renewable energy systems for power flow management in smart grid using an efficient hybrid technique. *Transactions of the Institute of Measurement and Control*, 2020, vol. 42, no. 11, pp. 2068-2087. doi: https://doi.org/10.1177/0142331220904818.

7. Boumassata A., Kerdoun D., Oualah O. Maximum power control of a wind generator with an energy storage system to fix the delivered power. *Electrical Engineering & Electromechanics*, 2022, no. 2, pp. 41-46. doi: https://doi.org/10.20998/2074-272X.2022.2.07.

8. Boutoubat M., Mokrani L., Machmoum M. Control of a wind energy conversion system equipped by a DFIG for active power generation and power quality improvement. *Renewable Energy*, 2013, vol. 50, pp. 378-386. doi: https://doi.org/10.1016/j.renene.2012.06.058.

9. Tang C.Y., Guo Y., Jiang J.N. Nonlinear Dual-Mode Control of Variable-Speed Wind Turbines With Doubly Fed Induction Generators. *IEEE Transactions on Control Systems Technology*, 2011, vol. 19, no. 4, pp. 744-756. doi: https://doi.org/10.1109/TCST.2010.2053931.

10. El-Sattar A.A., Saad N.H., El-Dein M.Z.S. Dynamic response of doubly fed induction generator variable speed wind turbine under fault. *Electric Power Systems Research*, 2008, vol. 78, no. 7, pp. 1240-1246. doi: https://doi.org/10.1016/j.epsr.2007.10.005.

11. Kahla S., Bechouat M., Amieur T., Sedraoui M., Babes B., Hamouda N. Maximum power extraction framework using robust fractional-order feedback linearization control and GM-CPSO for PMSG-based WECS. *Wind Engineering*, 2021, vol. 45, no. 4, pp. 1040-1054. doi: https://doi.org/10.1177/0309524X20948263.

12. Sahri Y., Tamalouzt S., Hamoudi F., Belaid S.L., Bajaj M., Alharthi M.M., Alzaidi M.S., Ghoneim S.S.M. New intelligent direct power control of DFIG-based wind conversion system by using machine learning under variations of all operating and compensation modes. *Energy Reports*, 2021, vol. 7, pp. 6394-6412. doi: https://doi.org/10.1016/j.egyr.2021.09.075.
13. Mazouz F., Belkacem S., Colak I., Drid S., Harbouche Y. Adaptive direct power control for double fed induction generator used in wind turbine. *International Journal of Electrical Power & Energy Systems*, 2020, vol. 114, art. no. 105395. doi: https://doi.org/10.1016/j.ijepes.2019.105395.
14. Zhi D., Xu L. Direct Power Control of DFIG With Constant Switching Frequency and Improved Transient Performance. *IEEE Transactions on Energy Conversion*, 2007, vol. 22, no. 1, pp. 110-118. doi: https://doi.org/10.1109/TEC.2006.889549.
15. Babes B., Hamouda N., Kahla S., Amar H., Ghoneim S.S.M. Fuzzy model based multivariable predictive control design for rapid and efficient speed-sensorless maximum power extraction of renewable wind generators. *Electrical Engineering & Electromechanics*, 2022, no. 3, pp. 51-62. doi: https://doi.org/10.20998/2074-272X.2022.3.08.
16. Wheeler P.W., Rodriguez J., Clare J.C., Empringham L., Weinstein A. Matrix converters: a technology review. *IEEE Transactions on Industrial Electronics*, 2002, vol. 49, no. 2, pp. 276-288. doi: https://doi.org/10.1109/41.993260.
17. Kolar J.W., Friedli T., Rodriguez J., Wheeler P.W. Review of Three-Phase PWM AC–AC Converter Topologies. *IEEE Transactions on Industrial Electronics*, 2011, vol. 58, no. 11, pp. 4988-5006. doi: https://doi.org/10.1109/TIE.2011.2159353.
18. Casadei D., Serra G., Tani A., Zarri L. Optimal Use of Zero Vectors for Minimizing the Output Current Distortion in Matrix Converters. *IEEE Transactions on Industrial Electronics*, 2009, vol. 56, no. 2, pp. 326-336. doi: https://doi.org/10.1109/TIE.2008.2007557.
19. Varajão D., Araújo R.E. Modulation Methods for Direct and Indirect Matrix Converters: A Review. *Electronics*, 2021, vol. 10, no. 7, art. no. 812. doi: https://doi.org/10.3390/electronics10070812.
20. Sayed M.A., Suzuki K., Takeshita T., Kitagawa W. PWM Switching Technique for Three-Phase Bidirectional Grid-Tie DC–AC–AC Converter With High-Frequency Isolation. *IEEE Transactions on Power Electronics*, 2018, vol. 33, no. 1, pp. 845-858. doi: https://doi.org/10.1109/TPEL.2017.2668441.
21. Shi T., Wu L., Yan Y., Xia C. Harmonic Spectrum of Output Voltage for Space Vector Pulse Width Modulated Ultra Sparse Matrix Converter. *Energies*, 2018, vol. 11, no. 2, art. no. 390. doi: https://doi.org/10.3390/en11020390.
22. Tuyen N., Dzung P. Space Vector Modulation for an Indirect Matrix Converter with Improved Input Power Factor. *Energies*, 2017, vol. 10, no. 5, art. no. 588. doi: https://doi.org/10.3390/en10050588.
23. Rodriguez J., Rivera M., Kolar J.W., Wheeler P.W. A Review of Control and Modulation Methods for Matrix Converters. *IEEE Transactions on Industrial Electronics*, 2012, vol. 59, no. 1, pp. 58-70. doi: https://doi.org/10.1109/TIE.2011.2165310.
24. Wang X., Lin H., She H., Feng B. A Research on Space Vector Modulation Strategy for Matrix Converter Under Abnormal Input-Voltage Conditions. *IEEE Transactions on Industrial Electronics*, 2012, vol. 59, no. 1, pp. 93-104. doi: https://doi.org/10.1109/TIE.2011.2157288.
25. Huber L., Borojevic D. Space vector modulation with unity input power factor for forced commutated cycloconverters. *Conference Record of the 1991 IEEE Industry Applications Society Annual Meeting*, 1991, pp. 1032-1041. doi: https://doi.org/10.1109/IAS.1991.178363.
26. Li D., Deng X., Li C., Zhang X., Fang E. Study on the space vector modulation strategy of matrix converter under abnormal input condition. *Alexandria Engineering Journal*, 2022, vol. 61, no. 6, pp. 4595-4605. doi: https://doi.org/10.1016/j.aej.2021.10.020.
27. Sellah M., Kouzou A., Mohamed-Seghir M., Rezaoui M.M., Kennel R., Abdelrahem M. Improved DTC-SVM Based on Input-Output Feedback Linearization Technique Applied on DOEWIM Powered by Two Dual Indirect Matrix Converters. *Energies*, 2021, vol. 14, no. 18, art. no. 5625. doi: https://doi.org/10.3390/en14185625.
28. Sahri Y., Tamalouzt S., Hamoudi F., Belaid S.L., Bajaj M., Alharthi M.M., Alzaidi M.S., Ghoneim S.S.M. New intelligent direct power control of DFIG-based wind conversion system by using machine learning under variations of all operating and compensation modes. *Energy Reports*, 2021, vol. 7, pp. 6394-6412. doi: https://doi.org/10.1016/j.egyr.2021.09.075.
29. Sun D., Wang X., Nian H., Zhu Z.Q. A Sliding-Mode Direct Power Control Strategy for DFIG Under Both Balanced and Unbalanced Grid Conditions Using Extended Active Power. *IEEE Transactions on Power Electronics*, 2018, vol. 33, no. 2, pp. 1313-1322. doi: https://doi.org/10.1109/TPEL.2017.2686980.
30. Chaudhuri A., Datta R., Kumar M.P., Davim J.P., Pramanik S. Energy Conversion Strategies for Wind Energy System: Electrical, Mechanical and Material Aspects. *Materials*, 2022, vol. 15, no. 3, art. no. 1232. doi: https://doi.org/10.3390/ma15031232.
31. Benbouhenni H., Lemdani S. Combining synergetic control and super twisting algorithm to reduce the active power undulations of doubly fed induction generator for dual-rotor wind turbine system. *Electrical Engineering & Electromechanics*, 2021, no. 3, pp. 8-17. doi: https://doi.org/10.20998/2074-272X.2021.3.02.
32. Benbouhenni H., Boudjema Z., Belaidi A. DPC Based on ANFIS Super-Twisting Sliding Mode Algorithm of a Doubly-Fed Induction Generator for Wind Energy System. *Journal Européen Des Systèmes Automatisés*, 2020, vol. 53, no. 1, pp. 69-80. doi: https://doi.org/10.18280/jesa.530109.

Received 22.08.2022
Accepted 10.11.2022
Published 06.05.2023

Aziz Boukadoum[1], *Associate Professor,*
Abla Bouguerne[1], *Associate Professor,*
Tahar Bahi[2], *Professor,*
[1] Labget laboratory, Department of Electrical Engineering,
Echahid Cheikh Larbi Tebessi University-Tebessa, Algeria,
e-mail: azizboukadoum@yahoo.fr (Corresponding Author),
bouguerneabla@yahoo.fr
[2] Department of Electrical Engineering,
University Badji Mokhtar Annaba, Algeria,
e-mail: tbahi@hotmail.fr

How to cite this article:
Boukadoum A., Bouguerne A., Bahi T. Direct power control using space vector modulation strategy control for wind energy conversion system using three-phase matrix converter. *Electrical Engineering & Electromechanics*, 2023, no. 3, pp. 40-46. doi: https://doi.org/10.20998/2074-272X.2023.3.06